RSC Advances

ROYAL SOCIETY OF CHEMISTRY

www.rsc.org/advances

ARTICLE

Received 00th January 20xx,

Accepted 00th January 20xx

DOI: 10.1039/x0xx00000x

www.rsc.org/

Chitosan supported silver nanowire as a platform for direct electrochemistry and highly sensitive electrochemical glucose biosensing†

Siva Kumar-Krishnan,[ab]* S. Chakaravarthy,[c] A. Hernandez-Rangel,[a] E. Prokhorov,[a] G. Luna-Bárcenas,[a] Rodrigo Esparza,[b] M. Meyyapan.[d]

The development of low-cost and sensitive glucose biosensor have been the focus of substantial research interest due to their diverse applications in medical diagnosis, healthcare, and environmental monitoring. Herein, we report the successful use of chitosan (CS) supported silver nanowires (AgNWs) based enzyme electrodes for highly sensitive electrochemical glucose biosensing. The glucose oxidase (GOx) enzyme is electrically contacted using highly conductive AgNWs and thereby significant enhancement in the direct electron transfer (DET) between the redox enzymes and the electrode surface. In addition, CS polymer matrix enables distinct self-assembly of GOx enzymes adjacent to the electrode surface, which further favours DET by increasing the charge transfer. Characterization by Fourier transform infrared (FTIR) spectroscopy and atomic force microscopy (AFM) measurements were used to evidence the intermolecular interaction and self-assembly of the GOx on CS polymers. AFM results clearly revealed that the self-assembly of the GOx on CS surfaces. The immobilized GOx exhibits a well-defined quasi-reversible redox peak with an electron rate constant (Ks) of 6.52 s^{-1} compared to the bare glassy carbon electrode (GCE). The resultant biosensor demonstrates a high sensitivity of 16.72 μA $mM^{-1}cm^{-2}$ with a wide linear range (1-15 mM), good selectivity and long-term stability for glucose detection. Our current approach represents a promising platform for the immobilization and electrical wiring of biomolecules with higher loading efficiency for designing low-cost, high sensitive enzymatic biosensors.

Introduction

The electrical wiring of redox enzymes with exceptional electrical contact with the electrode supports is of scientific importance as it provides a promising approach for the activation of bioelectrocatalytic systems of enzymes and facilitating direct electron transfer (DET) for highly sensitive amperometric biosensors[1] and biofuel cell applications.[2] Moreover, by achieving DET between redox enzyme and electrode one can overcome the various challenges associated with the use of redox mediator, toxicity, and limited stability. Different approaches have been investigated to improve the direct electrical communication of redox enzymes with the electrode surface including diffusional electron transfer mediators,[3] modification of cofactor units,[4] site-specific attachment of metal nanoparticles (NPs) with the enzyme cofactors,[5,6] immobilization of enzymes in redox polymers matrixes with the active functional groups,[7] and the reconstitution of apoenzymes on relay-cofactor units associated with the electrodes.[8] All these approaches allow modulating the DET characteristics. Recently, the self-assembly of GOx in a polymer/DNA scaffold and electrical wiring of redox-active cofactor, flavin adenine dinucleotide (FAD) through covalent coupling was shown to be an important strategy for enhancing the DET and the sensitivity of the biosensor.[7b,9]

Nanoscale materials such as nanowires and nanotubes have been well-recognized for the selective detection of biological species.[10] Several recent studies have focused on using metal/semiconductor nanoparticles, nanowires and carbon nanotubes (CNT) for highly effective redox mediators to facilitate the direct electron transfer between redox enzymes and electrode surfaces.[11] Several researchers have successfully exploited the attachment of conducting nanoparticles (NPs), such gold and diamond NP-enzyme hybrids, for tethering the deeply buried FAD cofactor unit of the GOx enzyme.[6,7d,9a] Also, *patholsky* et al.[11d] reported SWCNTs were used as a connector to the long range electrical wiring of the redox-active FAD cofactor unit. Similarly, anisotropic AgNPs such as nanoprisms[12] and nanoplates[13] have also been extensively examined for electrocatalytic oxidation of glucose on the electrode surface and thus more intimate/direct coupling with redox active centers. In particular, 1-D AgNWs are of special interest as potential DET systems due to their similar dimensions to the biomolecules and unique electronic properties.[14] Distinctive features of AgNWs such as high specific surface area, remarkable electrical conductivity, superior electrocatalytic properties and good affinity towards

[a] *Cinvestav Queretaro, Querétaro QRO, 76230, México. E-mail: skumar@fata.unam.mx Tel: +52-1-4422119921*
[b] *Centro de Física Aplicada y Tecnología Avanzada, Universidad Nacional Autónoma de México,Boulevard Juriquilla 3001, Santiago de Querétaro, Qro., 76230, México.*
[c] *Department of Nanoscience and nanotechnology CINVESTAV-IPN, ,DF CP 07360, México.*
[d] *NASA Ames Research Center, Moffett Field, CA 94035, USA.*

† Electronic Supplementary Information (ESI) available: SEM,TEM, UV-Vis, Comparison of different modified electrodes, Low detection limit and electrocatalytic activity towards H_2O_2. See DOI: 10.1039/x0xx00000x

biomolecules are ideal for constructing electrodes suitable for the effective detection of glucose.

In contrast, the enzyme immobilization strategies and their stability have been found to be the limiting factors for enhancing the enzymatic glucose sensing performance.[6,15] Numerous methods have been reported for immobilizing GOx on solid supports[7a,16] *via* direct adsorbing,[17] covalent anchoring[7b] or non-covalent functionalization[18] to protect the enzymes to remain stable while retaining their activities and providing an efficient electrical connection. Ideal immobilizing enzymes on the polymer matrix allow for large quantities of enzyme to be immobilized, provide a large surface area for the enzyme-substrate contact, increase stability and significantly reduce the electron-tunneling distance and overcome the diffusion problems.[7a] Recent studies have shown that the immobilized enzyme in the hydrophilic cavity dramatically improves its stability[19] than that of in hydrophobic cavity.[20] A variety of biodegradable polymers (e.g. hydrogels,[11b,21] elastomers,[22] poly lactic-co-glycolic acid (PLGA), polycaprolactone (PCL), polylactic acid (PLA) and poly (methacrylic acid)[23]) are used in the entrapment of the biomolecules as well as in the fabrication of biosensors. Among them, the CS is a hydrophilic biopolymer holds great promise as a versatile matrix material for the effective immobilization and promoting electron transfer of redox enzymes on the surface of modified electrodes due to the excellent biocompatibility, solubility in slightly acidic solution, higher stability, excellent film-forming ability and low-cost.[12,24] There have been limited studies on the combination of CS with AgNWs for glucose sensing.[14] However, self-assembly mechanism and direct electron wiring of redox enzymes by covalent attachment for significantly enhancing the DET characteristics have not been explored yet, and these are addressed here. Additionally, the development of biosensors with fast electron transfer rate, high sensitivity, stability, precise selectivity and low-cost still faces serious challenges for in-situ monitoring in a complex medium and miniaturization for commercial success.[25]

Herein, we report CS/AgNWs as an efficient immobilization and electrical wiring of GOx enzymes for the highly sensitive glucose biosensing. The results show that the hydrophilic CS can interact enzyme *via* -OH and -NH_3^+ side groups, which enable forming distinctive self-assembly network between the CS chains. Furthermore, the wiring of self-assembled GOx to the surface of the electrode was achieved using AgNWs through a covalent coupling that can enhance the charge transport and sensitivity for enzymatic electrochemical detection of glucose.

Experimental

Materials

Chitosan (medium molecular weight, Mw=300 kDa, 82% degree of deacetylation), silver nitrate ($AgNO_3$), Poly (vinyl pyrrolidone) (PVP, Mw of 55 000), glucose oxidase (GOx, from Aspergillus niger), glucose and ethylene glycol (EG) anhydrous (99.8%), L-ascorbic acid (≥99%), citric acid (≥99%), uric acid (≥99%), lactic acid (≥99%), sucrose (≥99%) and glutaraldehyde (50%) were purchased from Sigma-Aldrich. Acetic acid (glacial, 99-100%) was purchased from Merck. All reagents were analytical grade and used as received. Ultrapure water (18 MΩ·cm) was used for all experiments.

Synthesis of Ag nanowires

Uniform AgNWs were synthesized with a high yield by the modified polyol process.[26] Briefly, 0.204 g of $AgNO_3$ and 0.1332 g of PVP were dissolved in 5 ml of EG solvent separately. Both solutions were then simultaneously injected, dropwise for 5 minutes, into 25 ml of EG solvent, which was already being at 180^{o}C for 1 hr and under magnetic stirring. The solution has turned white after about a reaction time of 1 hr. The final colloidal suspension was then cooled to room temperature and subsequently washed, for several times with acetone and deionized water as well as by centrifuging a 10,000 rpm for 30 min to remove the excess PVP and unreacted Ag^+ ions. After that, the AgNWs were dispersed in 10 ml of sodium bicarbonate buffer solution (pH 9) and followed by addition of 1 ml of glutaraldehyde (50%) under magnetical stirring for further 2 hr for facilitating the covalent linkage of the GOx during the immobilization process.[9b] (See ESI, Fig. S1†) The nanowires were then separated and redispersed in deionized water for the preparation of the modified electrode.

Materials characterization

The formation of AgNWs was monitored by UV-Vis spectroscopy (UV-Vis spectrophotometer: Agilent 8453). The morphology of CS/AgNWs was analyzed by JEOM-JSM-7401F field-emission scanning electron microscope (FESEM) and also by JEOL-JEM-1010 transmission electron microscope (TEM) operated at 80 kV. X-ray diffraction (XRD) pattern were acquired using a Rigaku diffractometer ULTIMA IV, equipped with the CuKα radiation (λ=1.5406 Å). The interaction between the enzyme and the functional groups of CS was identified by FTIR spectroscopy on a Perkin Elmer spectrophotometer fitted with an ATR accessory in the range 4000-650 cm^{-1}. AFM images of the samples were acquired in a commercial SPM-AFM system (Bruker/Veeco/Digital Instruments Nanoscope IV Dimension 3100 system) at room temperature. The samples for the AFM measurement were prepared by drop casting 10 µL CS/GOx solutions on a cleaned silicon substrate and allowing the solution to dry at 4 ^{o}C. The topographic image was obtained using diamond-coated silicon AFM probe (Budget Sensors model ContDLC) with nominal length of 300 µm, in tapping mode at its resonant frequency of 13 kHz. The images were analyzed with Gwyddion software.

Preparation of CS/AgNWs/GOx-modified electrode

The glassy carbon electrodes (GCE) (d= 3 mm, homemade) were carefully polished with 1 and 0.3 µm alumina powder to obtain a mirror-finish surface and followed by sonication in water/ethanol mixture for 15 min. The cleaned electrodes were examined for reversible electron transfer, and subsequently, a 30 µL of PVP-coated AgNW dispersion was drop-casted on the surface of the pre-treated GCE and left to dry at room temperature to obtain an AgNW-modified GCE. The covalent attachment of GOx on the surface of the AgNW-GCE was obtained by addition of 5 µL of GOx (30 mg mL^{-1}) to

the 2 µL of CS and then drop-casted onto the resultant AgNW-GCE and dried at 4 °C at least for 4 hr. Removal of the non-bounded GOx on the resultant enzyme-modified electrode was carried out by rinsing with water followed by drying. The enzyme-modified electrode was stored in a refrigerator at 4 °C when not in use.

Electrochemical measurements

We performed all the electrochemical experiments by employing a standard three-electrode electrochemical cell (VoltaLab 40 PGZ 301) with the Platinum foil as the auxiliary electrode and a saturated calomel electrode (SCE) as the reference one. The working electrodes were homemade glassy carbon electrodes. The glucose sensing performance of the modified electrodes was carried out using cyclic voltammetry (CVs) measurements and the cyclic voltammograms were recorded in 0.1 M PBS (pH 7.4) in O_2-saturated conditions in the presence of different concentration of glucose.

Results and discussion

Structural characterization

We examined the structural and morphological features of the as-prepared AgNWs by electron microscopes. FESE micrographs uncovered the high-yield formation of uniform nanowires with an average diameter of 50-70 nm, a length of 3-15 µm and resulted in pentagonal cross-sections (Fig. S2†). The pentagonally-twined structure can form due to the existence of five {111} twin planes that cross along the line in the center of each nanowire.[27] Additionally, the low-resolution TEM images reveal that the high-density AgNWs are well dispersed in the CS *via* electrostatic interactions (Fig. 1a). High-resolution TEM (Fig. 1b) shows the periodic lattice fringes with a measured interplanar distance of 0.236 nm, which corresponds well to the {111} planes of Ag.[28] HR-TEM analysis confirms the growth of AgNWs that is mainly oriented to {111} planes (Fig. S3†). Also, UV-vis and X-ray diffraction (XRD) analyses further confirm the formation of AgNWs. UV-vis spectra show two distinct surface plasmon resonance (SPR) characteristic absorption peaks at 350 and 429 nm (Fig. S4†).[29] The intense peak at 429 nm represents the transverse plasmon resonance whereas the weaker one (at 352 nm) corresponds to the quadrupole resonance excitation of nanowires.[30] Figure 1c shows the XRD pattern of CS/AgNWs displaying sharp peaks at 2θ values of 38.0, 44.20, 64.30 and 77.70 degrees that correspond to (111), (200), (220) and (311) planes of the face-centered cubic (fcc) structure of Ag, respectively.[27] Notably, the high-intensity diffraction peak at the 2θ value of 38.0 indicates that AgNWs may have a preferred orientation along the (111) crystalline plane.[27]

FTIR analysis was done to obtain the specific interaction and effectiveness in enzyme immobilization on the CS/AgNWs films. Fig. 1d shows representative FTIR spectra of pure GOx, CS/AgNWs, and CS/AgNWs/GOx. The pure GOx exhibits three characteristic transmittance peaks at 1658, 1542 and 1103 cm^{-1} corresponding to the adsorptions of amide I and amide II, and the C-O stretching vibration of GOx, respectively.[31] The CS/AgNWs composite has peaks at 1643 cm^{-1} band for amide I (C=O stretching); 1556 cm^{-1} for amide II

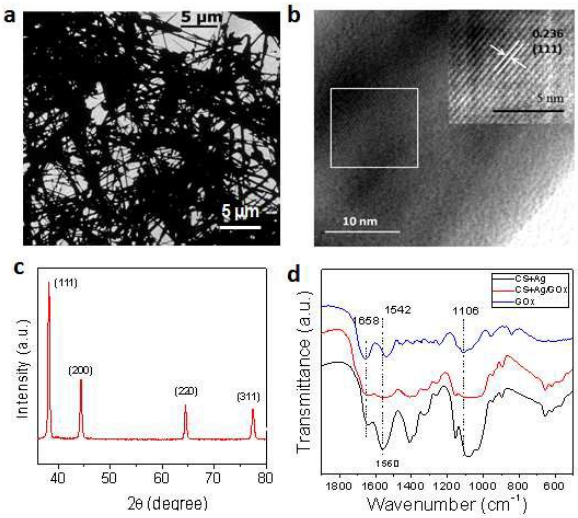

Fig 1. (a) Low and b) high-resolution TEM images of CS/AgNW. The inset shows the magnified version of the marked section. (c) XRD pattern of the as-prepared CS/AgNWs. (d) FTIR spectra of CS/AgNWs, CS/AgNWs/GOx, and GOx, respectively

(N-H bending); bands at 1410 cm^{-1} for OH bending vibrations.[32] After immobilization of GOx on the CS/AgNWs, both amide I and amide II peaks of GOx newly appear, indicating the effective immobilization of GOx on the CS/AgNWs by retaining its secondary structure. We ascribe this effective immobilization of GOx due to the combination of two components: i) the linkage of GOx to the nanowires. and, ii) the presence of biocompatible CS that may allow to maintain the native structure of GOx and stabilize them, thus preventing the enzyme denaturation.[12]

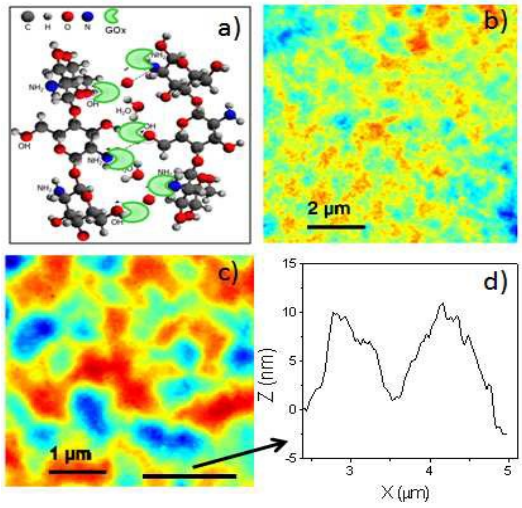

Fig 2. a) Schematic of the interaction between GOx and the CS biopolymer matrix and their assembly network between the CS chains through -OH and $–NH_3^+$ functional groups. b) Tapping mode AFM topographic images of b) low and c) high magnification images of self-assembled immobilized GOx in the CS matrix, and d) cross-sectional analysis.

The effective coupling of GOx with the adjacent -OH and -NH_3^+ groups of the CS leads to the formation of self-assembled networks between the CS chains as depicted in Fig. 2a. Furthermore, our AFM measurements affirm the self-organization of GOx in the CS matrix as shown in the Fig. 2b and c. The measured height of individual GOx is ca. 9 nm (Fig. 2d), that is consistent with the previously reported dimensions of the GOx in protein scaffolds.[1a,9a] These self-assembled GOx interacts with the AgNWs *via* the covalent coupling.[9b] The covalent linkage of GOx on the surface of the AgNWs can prevent the non-specific coupling on the nanowires as well as electrically wires the redox active centre of the enzyme to the electrode surface.[11d]

Direct electrochemistry and amperometric detection of glucose using CS/AgNWs/GOx-modified electrode.

The direct electron transfer of the CS /AgNWs/GOx-modified glassy carbon electrode (GCE) was investigated using cyclic voltammetry (CV). The comparison of bare GCE, CS/AgNWs/GCE, and CS/AgNWs/GOx/GCE modified electrode (Fig. S5†). Notably, the bare GCE and the CS/AgNWs/GCE electrode did not show any peak over the measured potential range, suggesting that these modified electrodes are electrochemically inactive. Nevertheless, the CS/AgNWs/GOx/GCE enzyme electrode exhibits two well-defined redox peaks of the electrochemical oxidation/reduction process of the immobilized GOx structure.[11c] This electrode undergoes a quasi-reversible redox reaction during the CV cycle. Fig. 3a shows the CVs of enzyme based CS/AgNWs/GOx- modified GCE electrode as a function of scan rate recorded in a phosphate buffered solution (PBS, pH 7.4) under N_2-saturated conditions. The anodic peak shifts towards a more positive potential while the cathodic peak shifts towards a more negative potential. Moreover, the peak currents increase linearly with the scan rate from 20 to 500 mVs^{-1} (Inset of Fig. 3a), clearly suggesting a surface-controlled electrochemical oxidation/reduction process of the bounded GOx structure.[33] We calculated the electron transfer rate constant (ks) for the modified electrode for scan rates higher than 500 mVs^{-1} according to the Lavirons equation.[34]

$$\log K_s = \alpha\log(1-\alpha)+(1-\alpha)\log\alpha-\log(RT/nFv) - \alpha(1-\alpha)nF\Delta E_p/2.3RT \quad (1)$$

Where α is the charge transfer coefficient (~ 0.5), R is the universal gas constant (8.314 J mol^{-1} K^{-1}), T is the room temperature (298 K), and ΔEp is the redox peak separation. The calculated value of ks is 6.52 s^{-1} that is higher than that for the graphene-GOx (4.8 s^{-1}),[35] mesoporous 1D hydroxyapatite on reduced graphene oxide (3.50 s^{-1}),[36] MWCNT-GOx (1.56 s^{-1})[37] TiO_2-coated CNT (3.5 s^{-1})[38a] and PANI nanotube-GOx (3.0 s^{-1})[38b] biosensors. The observed larger value of ks for the CS/AgNWs/GOx indicates the higher affinity and fast direct electron-transfer between the immobilized GOx and the electrode surface. Fig. 3b depicts the measured CVs for the modified GCE electrode in the presence of different concentrations of glucose (1-13 mM) in 0.1 M PBS solution (pH 7.4) under O_2-saturation conditions. The electrode displays a strong reduction peak around -0.65 V and the electrocatalytic

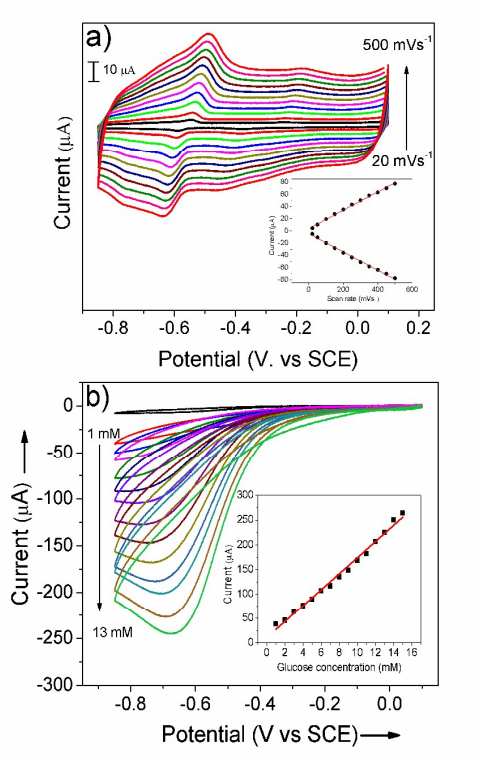

Fig 3. (a) Cyclic voltammograms of the CS/AgNWs/GOx-GCE at scan rates ranging from 20 to 250 mVs^{-1}, recorded in 0.1 M PBS (pH 7.4) under N_2 saturated condition. The inset shows the linear dependence of peak current vs. scan rate. (b) Cyclic voltammograms of CS/AgNWs/GOx-GCE in 0.1 M PBS (pH 7.4) with successive addition of glucose. The inset shows the calibration plot with the measured glucose concentrations.

anodic current increases upon sequential addition of glucose. The linear extrapolation of current as a function of glucose concentration (1-15 mM) yields a sensitivity of 16.72 μA mM^{-1} cm^{-2}. The observed electrocatalytic cathodic and anodic peak separation at the redox potential of the modified electrode further imply that the covalent linkage communicates the FAD co-factor unit of the GOx with the electrode surface.[8b] Our biosensor demonstrates a wide linear range (1-15 mM) broader than the typical glucose concentration in human blood (ca. 5 mM).[7a] Moreover, the sensor exhibits an excellent linear relationship between current and glucose concentration with a regression coefficient (R^2) of 0.991 in the low concentration regime ranging from 2.1 μM-100 μM (Fig. S6†).

To determine the optimal concentration of immobilized GOx on the modified electrodes, we carried out experiments with a different initial concentration of GOx (mg/ml) and estimated the sensitivity to detect glucose of the different electrodes. Fig. 4a shows the calibration plots obtained for glucose determination of the modified electrodes containing different GOx concentrations. Fig. 4b displays the sensitivity values of the different electrodes versus the GOx concentration. The results demonstrate that the sensitivity increases with GOx concentration and reaches a maximum value of about 30 mg/ml of GOx. Above this critical concentration, the sensitivity

is dramatically decreased. In the low GOx concentration region, the availability of immobilized enzyme may be limited. The significant reduction in sensitivity at higher concentrations could most likely be due to the uncoupled excess GOx with the CS/AgNWs. Therefore, the optimum concentration of GOx is found to be 30 mg/ml that gives higher sensitivity. Fig. 5 depicts the schematic illustration of CS/AgNWs/GOx-GCE modified electrode and the processes occurring during the enzymatic electrochemical glucose detection.

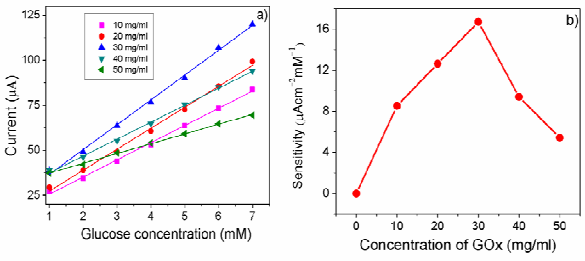

Fig 4. (a) Calibration curves for glucose obtained from CVs of modified electrode with different GOx concentrations. (b) Dependence of glucose sensitivity for various concentrations of GOx immobilized on the CS/AGNWs-GOx modified electrode.

The possible mechanism of electrocatalytic reduction can be expressed by the following reactions in the presence of O_2.

$$glu\cos e + GO_x(FAD) \rightarrow gluconolactone + GO_x(FADH_2)$$
$$GO_x(FADH_2) + O_2 \rightarrow GO_x(FAD) + H_2O_2 \quad (2)$$

The FAD active site of GOx reacts with glucose and converts into gluconolactone and $FADH_2$ (FAD and $FADH_2$ are the oxidized and reduced forms of flavin adenine dinucleotide). Subsequently, the $FADH_2$ is reoxidized by the oxygen present in the solution, the two electrons are transferred through the FAD cofactor to O_2, consequently generating hydrogen peroxide (H_2O_2). As a result, the sensitivity of the modified electrode can be evaluated by detecting the electric current generated by the enzymatic reaction.[11b,21,33,39] The AgNWs play a vital role as efficient catalyst, significantly enhancing the performance of the biosensor. The electrocatalytic activity of the CS/AgNWs-modified electrode as a function of H_2O_2 concentration indicates that the current increases linearly with H_2O_2 concentration (Fig. S7†). Homogeneous dispersion of nanowires on the GCE electrode surface greatly reduces the diffusion distance of the H_2O_2 molecules due to the significantly higher catalytic ability of the AgNWs.[11b] Therefore, the enzymatically-liberated H_2O_2 is catalyzed by the nanowires with the charges transferred to the electrode surface, thereby increasing the output current and the sensitivity of the glucose sensor. Table 1 shows the comparative performance of our biosensor with other reported electrochemical biosensors based on different nanomaterials.[10b,11c,14,40] The observed remarkable sensitivity of 16.72 μA $mM^{-1}cm^{-2}$, a wide linear range (1-15 mM) and significantly lower detection limit of limit

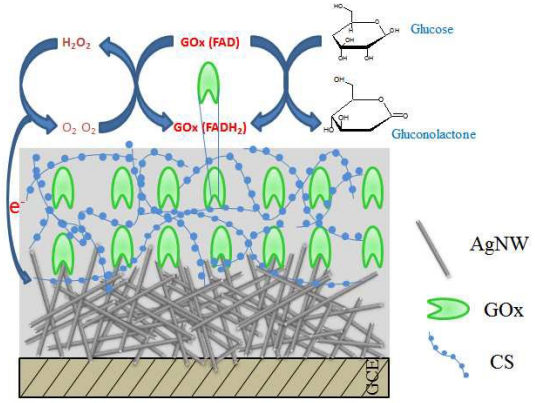

Fig 5. The Schematic illustration of CS/AgNWs/GOx-GCE modified electrode and the process occurring during the enzymatic electrochemical glucose sensing.

of 2.1 μM our modified electrode is relatively better. This performance enhancement can be attributed to a number of factors; firstly to the appreciable higher electrical conductivity of the AgNWs, which electrically connects the active site of the redox protein to the electrode surface thereby providing the necessary direct electrical communication. Secondly, the strong electrostatic interaction between -OH and $-NH_3^+$ groups of the CS and the GOx could form an internally stable and distinct self-assembled network that allow high loading capacity to immobilize active GOx adjacent to the electrode surface, that further shorten the electron tunneling distance between the electrode surface and the immobilized GOx. Finally, the highly biocompatible CS could effectively stabilize enzymes, which can effetively prevent the enzyme from denaturation and enhance the life-time. Overall, the above results provide unambiguous evidence for the DET mechanism in the biosensor; that is significantly enhanced by the formation of the electrical wiring and self-assembly of the redox enzymes.

Stability and interference studies of the biosensor

We investigated further the stability of the modified electrode by amperometric measurements in the presence of 5 mM glucose in O_2-saturated PBS solution (pH 7.4). The current response of the biosensor in Fig. 6a shows 76% retention of the original response over a 7 day period (stored at -4°C), indicating excellent stability of the fabricated sensor. To verify the selectivity of the modified electrode, the CVs for glucose determination were carried out with common interfering species. Fig. 6b shows a significant current response with the addition of 1 mM glucose and almost negligible current change with 1 mM of ascorbic acid (AA), citric acid (CA), lactic acid (LA), uric acid (UA) and sucrose. This results confirms that the present biosensor is not significantly affected by the interfering agents, added here at higher concentrations than their normal levels in blood suggesting the excellent selectivity of the biosensor. The good selectivity is attributed due to the

Table 1. Comparison of the analytical performance of different glucose biosensors.

Modified electrodes	Sensitivity ($\mu A\ mM^{-1}\ cm^{-2}$)	Linear range (mM)	Detection limit (μM)	Ref.
AgNWs/CS/GOx	16.72	1-15	2.1	This work
AgNW/CS-GOx	N/A	0.010 to 0.8	2.83	14b
TNT/AuNPs/GOx	5.1	0.01 to 1.2	N/A	40a
SiNWs@AuNPs-GOx	N/A	1-16	50	40b
PtNWAE/GOx	4.21	0.083 -182	83.23	40c
1DHS TiO_2/GOx	9.90	0.15 -1.5	1.29	11c
GR–CNT@ZnO–GOx	5.36 (±0.072)	0.01-6.5	4.5	40d
CNT-GOx	N/A	1-30	80.0	10b
GR-GOx	1.85	0.01-27	10	35
RGO/Hap-GOx	16.9	0.1-11.5	30	36
GR/AuNPs/CS-GOx	0.55	2-10	180	40e
PLL/RGO/ZrO_2-GOx	11.65	0.29-14	130	40f

NW: nanowire; PtNWAE platinum nanowire array electrode; 1DHS one-dimensional hierarchically structured; CNT carbon nanotubes; GR graphene; RGO Reduced graphene oxide; TNT: Titanate nanotube; PLL: Poly (L-lysine), N/A: not available

fact that, GOx functionalized CS/AgNWs can selectively undergo enzymatic reaction by catalytic oxidation of D-glucose and fast conversion into D-gluconolactone and H_2O_2.[33] Whereas with other interferncing species such as AA, CA, LA, UA and sucrose, that cannot undergo enzymatic reaction. As a result, the electrons are passed towards the electrode surface through AgNWs, and the currernt changes when addition of glucose. Hence, our result suggest that the CS/AgNWs/GOx biosensor platform have a good stability and anti-interference ability.

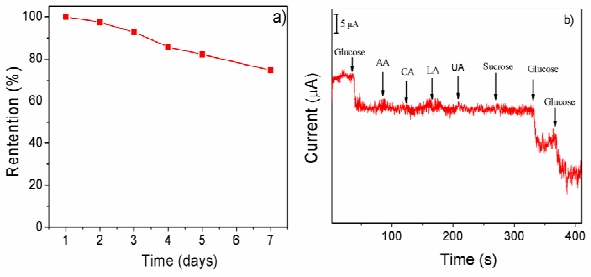

Fig 6. (a) The stability of the CS/AgNWs/GOx-GCE modified electrode over a week storage period. (b) The amperometric response is showing the effect of interfering substances (1 mM of AA, CA, LA, UA, sucrose, and glucose, respectively.

Conclusions

In summary, we present GOx-functionalized CS supported AgNWs as sensitive glucose biosensor. We also describe a new strategy to self-assembly and electrically wiring of redox enzymes based on CS/AgNWs that provide the enhanced DET between GOx enzyme and the electrode surface. The self-assembly of enzymes in the CS increases the effective immobilization adjacent to the electrode surface and highly conductive AgNWs serve as the connector to facilitate DET between the FAD co-factor and the electrode surface, thus effectively improving the sensitivity of the biosensor. AFM analysis confirms the self-assembled nature of GOx in the side chains of CS. Also, our experimental findings demonstrate that the developed biosensor exhibits unprecedented performance in sensing glucose with high sensitivity values of 16.72 $\mu A\ mM^{-1}\ cm^{-2}$, linear range of 1-15 mM, and excellent stability and selectivity. The excellent performance achieved here is due to the combined advantage of distinct self-assembly of the immobilized GOx on the biocompatible CS and the electrical wiring using highly conductive AgNWs, which enables enhanced charge transport between the GOx and electrode surface. Besides, 1D morphology of the AgNWs also favours the higher affinity towards biomolecules, and mass transfer thereby improves the sensitivity of the glucose biosensor. Our present approach provides a promising platform for the development of low-cost, highly sensitive enzyme-based biosensors and biofuel cell applications.

Acknowledgements

The authors are grateful to J. A. Munoz-Salas for assistance in the construction of GCE electrodes, Ma. Lourdes Palma Tirado

(Campus UNAM Juriquilla, Qro) for TEM measurements and C.I. Enriquez-Flores for the help in AFM measurements.

Notes and references

1 (a) O. I. Wilner, Y. Weizmann, R. Gill, O. Lioubashevski, R. Freeman and I. Willner, *Nat. Nanotechnol.*, 2009, **4**, 249; (b) T. Nöll and G. Nöll, *Chem. Soc. Rev.*, 2011, **40**, 3564; (c) B. J. Johnson, W. Russ Algar, A. P. Malanoski, M. G. Ancona and I. L. Medintz, *Nano Today*, 2014, **9**, 102.
2 (a) X. Jiang, J. Hu, A. M. Lieber, C. S. Jackan, J. C. Bi, L. A. Fitzgerald, B. R. Ringeisen and C. M. Lieber, *Nano Lett.*, 2014, **14**, 6737; (b) S. K. Chaudhuri and D. R. Lovley, *Nat. Biotechnol.*, 2003, **21**, 1229.
3 P. Janda and J. Weber, *J. Electroanal. Chem. Interfacial Electrochem.*, 1991, **300**, 119.
4 Riklin, E. Katz, I. Willner, A. Stocker and A. F. Bückmann, *Nature*, 1995, **376**, 672.
5 A. Heller, *Nat. Biotechnol.*, 2003, **21**, 631.
6 J. T. Holland, C. Lau, S. Brozik, P. Atanassov and S. Banta, *J. Am. Chem. Soc.*, 2011, **133**, 19262.
7 (a) C. R. Parthasarathy, R. V., Martin, *Nature*, 1994, **369**, 298; (b) A. A. Reitinger, N. A. Hutter, A. Donner, M. Steenackers, O. A. Williams, M. Stutzmann, R. Jordan and J.A. Garrido, *Adv. Funct. Mater.*, 2013, **23**, 2979.
8 (a) M. Zayats, E. Katz and I. Willner, *J. Am. Chem. Soc.*, 2002, **124**, 2120; (b) A. Trifonov, K. Herkendell, R. Tel-Vered, O. Yehezkeli, M. Woerner and I. Willner, *ACS Nano*, 2013, **7**, 11358.
9 (a) M. Frasconi, A. Heyman, I. Medalsy, D. Porath, F. Mazzei and O. Shoseyov, *Langmuir*, 2011, **27**, 12606; (b) L. Rodríguez-Lorenzo, R. de la Rica, R. A. Álvarez-Puebla, L. M. Liz-Marzán and M. M. Stevens, *Nat. Mater.*, 2012, **11**, 604. (c) J. Lee, H. Ahn, I. Choi, M. Boese and M. J. Park, *Macromolecules*, 2012, **45**, 3121.
10 (a) Y. Cui, Q. Wei, H. Park and C. M. Lieber, *Science*, 2001, **293**, 1289; (b) Y. Lin,F. Lu, Y. Tu, Z.F. Ren, *Nano Lett.*, 2004, **4**, 191.
11 (a) A. Chen and S. Chatterjee, *Chem. Soc. Rev.*, 2013, **42**, 5425; (b) D. Zhai, B. Liu, Y. Shi, L. Pan, Y. Wang, W. Li, R. Zhang and G. Yu, *ACS Nano*, 2013, **7**, 3540; (c) P. Si, S. Ding, J. Yuan, X. W. Lou and D. H. Kim, *ACS Nano*, 2011, **5**, 7617; (d) F. Patolsky, Y. Weizmann and I. Willner, *Angew. Chemie - Int. Ed.*, 2004, **43**, 2113.
12 W. Shi and Z. Ma, *Biosens. Bioelectron.*, 2010, **26**, 1098.
13 C. L. Lee, H. L. Yang, C. W. Chen and Y. L. Tsai, *Electrochim. Acta*, 2013, **106**, 411.
14 (a) X. Yang, J. Bai, Y. Wang, X. Jiang and X. He, *Analyst*, 2012, **137**, 4362; (b) L. Wang, X. Gao, L. Jin, Q. Wu, Z. Chen and X. Lin, *Sensors Actuators, B Chem.*, 2013, **176**, 9.
15 S. Boland, F. Barriere and D. Leech, *Langmuir*, 2008, **24**, 6351.
16 (a) L. Li, Y. Shi, L. Pan, Y. Shi and G. Yu, *J. Mater. Chem. B*, 2015, **3**, 2920; (b) S. Patra, T. Hidalgo-Crespo, A. Permyakova, C. Sicard, C. Serre, A. Chausse, N. Steunou, L. Legrand, *J. Mater. Chem. B*, 2015, 3, 8983.
17 M. E. G. Lyons and G. P. Keeley, *Chem. Commun.*, 2008, 2529.
18 J. S. Y. Chia, M. T. T. Tan, P. S. Khiew, J. K. Chin and C. W. Siong, *Sensors Actuators B Chem.*, 2015, **210**, 558.
19 J. Grimaldi, M. Radhakrishna, S. K. Kumar and G. Belfort, *Langmuir*, 2015, **31**, 1005.
20 M. Radhakrishna, J. Grimaldi, G. Belfort and S. K. Kumar, *Langmuir*, 2013, **29**, 8922.
21 L. Li, Y. Wang, L. Pan, Y. Shi, W. Cheng, Y. Shi and G. Yu, *Nano Lett.*, 2015, **15**, 1146.
22 S. Hwang, C. H. Lee, H. Cheng, J. Jeong, S.-K. Kang, J. Kim, J. Shin, J. Yang, Z. Liu, G. a. Ameer, Y. Huang and J. a. Rogers, *Nano Lett.*, 2015, **15**, 2801.
23 S. W. Hwang, J. K. Song, X. Huang, H. Cheng, S. K. Kang, B. H. Kim, J. H. Kim, S. Yu, Y. Huang and J. a. Rogers, *Adv. Mater.*, 2014, **26**, 3905.
24 (a) S. T. Koev, P. H. Dykstra, X. Luo, G. W. Rubloff, W. E. Bentley, G. F. Payne and R. Ghodssi, *Lab Chip*, 2010, **10**, 3026; (b) M. Sheng, Y. Gao, J. Sun and F. Gao, *Biosens. Bioelectron.*, 2014, **58**, 351. (c) C. Zhao, Y. Meng, C. Shao, L. Wan, K. Jiao, *Electroanalysis* 2008, **20**, 520.
25 V. Scognamiglio, *Biosens. Bioelectron.*, 2013, **47**, 12.
26 X. Zeng, B. Zhou, Y. Gao, C. Wang, S. Li, C. Y. Yeung and W. Wen, *Nanotechnology*, 2014, **25**, 495601.
27 Y. Sun, Y. Ren, Y. Liu, J. Wen, J. S. Okasinski and D. J. Miller, *Nat. Commun.*, 2012, **3**, 971.
28 Y. Xiong, Y. Xie, C. Wu, J. Yang, Z. Li and F. Xu, *Adv. Mater.*, 2003, 405.
29 J. J. Mock, S. J. Oldenburg, D. R. Smith, D. a. Schultz and S. Schultz, *Nano Lett.*, 2002, **2**, 465.
30 Y. Sun, B. Gates, B. Mayers and Y. Xia, *Nano Lett.*, 2002, **2**, 165.
31 (a) J. Tang, Y. Wang, J. Li, P. Da, J. Geng and G. Zheng, *J. Mater. Chem. A*, 2014, **2**, 6153; (b) S. J. Bao, C. M. Li, J. F. Zang, X. Q. Cui, Y. Qiao and J. Guo, *Adv. Funct. Mater.*, 2008, **18**, 591.
32 S. Kumar-Krishnan, E. Prokhorov, M. Hernández-Iturriaga, J. D. Mota-Morales, M. Vázquez-Lepe, Y. Kovalenko, I. C. Sanchez and G. Luna-Bárcenas, *Eur. Polym. J.*, 2015, **67**, 242.
33 K. Kwak, S. S. Kumar, K. Pyo and D. Lee, *ACS Nano*, 2014, **8**, 671.
34 E. Laviron, *J. Electroanal. Chem. Interfacial Electrochem.*, 1979, **101**, 19.
35 B. Unnikrishnan, S. Palanisamy and S. M. Chen, *Biosens. Bioelectron.*, 2013, **39**, 70.
36 G. Bharath, R. Madhu, S.-M. Chen, V. Veeramani, a. Balamurugan, D. Mangalaraj, C. Viswanathan and N. Ponpandian, *J. Mater. Chem. B*, 2015, **3**, 1360.
37 (a) C. Cai and J. Chen, *Anal. Biochem.*, 2004, **332**, 75.
38 M. Tasviri, H. A. Rafiee-Pour, H. Ghourchian and M. R. Gholami, *J. Mol. Catal. B Enzym.*, 2011, **68**, 206. (b) L. Zhang, C. Zhou, J. Luo, Y.Long, C. Wang, T. Yu, D. Xiao., *J. Mater. Chem. B*, 2015, **3**, 1116.
39 X. Jiang, C. Sun, Y. Guo, G. Nie and L. Xu, *Biosens. Bioelectron.*, 2015, **64**, 165.
40 (a) R. Zhao, X. Liu,J. Zhang, J.Zhu, D.K.Y.Wang, *Electrochem. Acta*.,2015, 163, 64.(b) S. Su, Y. He, S. Song, D. Li, L. Wang, C. Fan and S.-T. Lee, *Nanoscale*, 2010, **2**, 1704; (c) Y. Wang, Y. Zhu, J. Chen and Y. Zeng, *Nanoscale*, 2012, **4**, 6025; (d) K.-Y. Hwa and B. Subramani, *Biosens. Bioelectron.*, 2014, **62**, 127. (e) C. Shan, H. Yang, D. Han, Q. Zhang, A. Ivaska and L. Niu, *Biosens. Bioelectron.*, 2010, **25**, 1070. (f) A. T. Ezhil Vilaan, S. M. Chen, M. Ajmal Ali and F. M. A. Al-Hemaid, *RSC Adv.*, 2014, **4**, 30358.

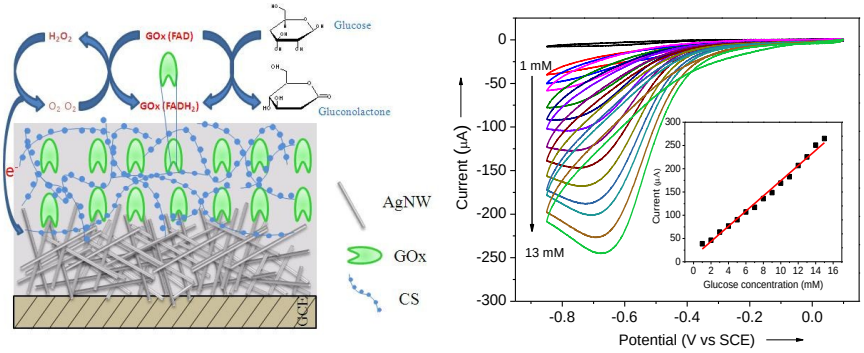

Chitosan supported silver nanowire (CS/AgNWs) based enzyme electrodes for highly sensitive glucose sensing